

# A Domain Decomposition Method for Heterogeneous Reservoir Flow

Brit Gunn Ersland <sup>1</sup> and Magne S. Espedal <sup>2</sup>

## ABSTRACT

The main objective for this work is to study two phase flow (oil, water) in a heterogeneous porous media.

To solve the elliptic pressure equation we use a finite element formulation, while the velocity is calculated in a flux conserving manner from the pressure. For the parabolic saturation equation we use a two step operator splitting procedure [EE87].

Our computational domain consist of two regions with different physical properties. Domain decomposition is used for adaptive refinement, and to treat the interior boundary. We present an iteration procedure which ensure conservation of mass.

## MODEL PROBLEM

For incompressible immiscible displacement of oil by water in a reservoir the following equations yield

$$\nabla \cdot \mathbf{v} = q_1(\mathbf{x}, t) \quad (1)$$

$$\mathbf{v} = -\mathbf{K}(\mathbf{x})M(S, \mathbf{x}) \cdot \nabla p \quad (2)$$

$$\phi \frac{\partial S}{\partial t} + \nabla \cdot (f(S)\mathbf{v}) - \epsilon \nabla \cdot (D(S, x)\nabla S) = q_2. \quad (3)$$

---

<sup>1</sup> Department of Mathematics, University of Bergen, Johs. Brunsg. 12., 5008 Bergen, Norway, email: resbg@mi.uib.no

<sup>2</sup> Department of Mathematics, University of Bergen, Johs. Brunsg. 12., 5008 Bergen, Norway, email: resme@mi.uib.no

We will use Neumann type of boundary conditions.

$\mathbf{v}$  is the total Darcy velocity, which is the sum of the velocity of the oil and water phase.  $\mathbf{K}(\mathbf{x})$  is the permeability which depend on the porous medium,  $M(S, \mathbf{x})$  is a mobility function that depend on the water saturation  $S$ , and  $p$  is the total fluid pressure.  $\phi$  is the porosity of the porous media which is considered constant. The fractional flow function  $f(S)$  is a nonlinear function of the saturation and is given as

$$f(S) = \frac{\lambda_w(S)}{\lambda_w(S) + \lambda_o(S)} \quad (4)$$

where the mobility of oil and water,

$$\lambda_l, l \in \{o, w\}$$

is a given function of  $S$ .

The diffusion coefficient  $D(S, x)$  is

$$D(S, x) = K(x)f(S)\lambda_o(S)\frac{\partial P_c}{\partial S}. \quad (5)$$

$K(x)$  is the absolute permeability and  $P_c$  is the capillary pressure function. It is well known that a nonlinear equation like eq(3) will establish shock like solutions therefore we split the function  $f(S)$  into two parts. [EE87] [DR82]

$$f(S) = \bar{f}(S) + b(S)S,$$

The convective part

$$\phi \frac{\partial S}{\partial \tau} \equiv \frac{\partial S}{\partial t} + \bar{f}'(S)\mathbf{v} \cdot \nabla S = 0, \quad (6)$$

is solved by the Modified Method of Characteristics [DR82]. The elliptic part

$$\phi(\mathbf{x}) \frac{\partial S}{\partial \tau} + \nabla \cdot (b(S)S\mathbf{v}) - \nabla \cdot (D(S, \mathbf{x}) \cdot \nabla S) = 0 \quad (7)$$

is discretised by bilinear finite elements, with optimal testfunctions [BM84]. The nonlinear terms in the elliptic equation is linearised around the solution of the convective equation.

The pressure equation is solved by an finite element method with bilinear elements and chapau testfunctions. The velocity is derived from the pressure with a second order method.

We use a sequential time-stepping procedure decribed in [DES92].

## COMPUTATIONAL DOMAIN

Our computational domain consist of two regions with different physical properties. The first region has permeability  $K_1$  and capillary pressure curve  $P_{C1}$ , the second has permeability  $K_2$  and capillary pressure curve  $P_{C2}$ .

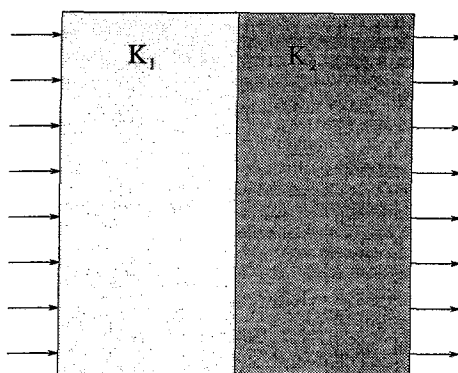


**Figure 1** Computational domain showing two different regions with different physical properties connected through an interior boundary.

The capillary pressure function,

$$P_C(S) = 0.09\phi^{-0.9}K^{-0.1}\frac{1-S}{\sqrt{S}} \tag{8}$$

depend on the saturation  $S$  and the permeability  $K$  [KME92]. Further,

$$\lambda_l = S_l^2, \quad l \in \{o, w\}$$

in both regions.

In addition to our outer Neumann boundary condition, the discontinuity in  $\mathbf{K}$ , leads to a problem with the interior boundary condition. The capillary pressure must be continuous over the interior boundary  $\Gamma$ .

$$P_{C_1}(S_1) = P_{C_2}(S_2) \tag{9}$$

This condition lead to a discontinuous saturation over the boundary.

$$S_1 \neq S_2 \tag{10}$$

In order to conserve the mass over the boundary the flux must be conserved over the interior boundary  $\Gamma$ .

$$(f(S)\mathbf{v} - \epsilon D \cdot \nabla S)^1 \cdot \mathbf{n}^\Gamma = (f(S)\mathbf{v} - \epsilon D \cdot \nabla S)^2 \cdot \mathbf{n}^\Gamma \tag{11}$$

## DOMAIN DECOMPOSITION

In order to solve our equations on the computational domain, we construct a coarse grid  $\Omega_C$ , where the interior boundary is in the middle of a set of coarse grid elements. In addition we construct a fine grid  $\Omega_F$ , where the interior boundary is placed in

a set of nodes. The fine grid is decomposed into the same number of overlapping subgrids as there are elements in the coarse grid. We may write

$$\Omega_F = \cup \Omega^i.$$

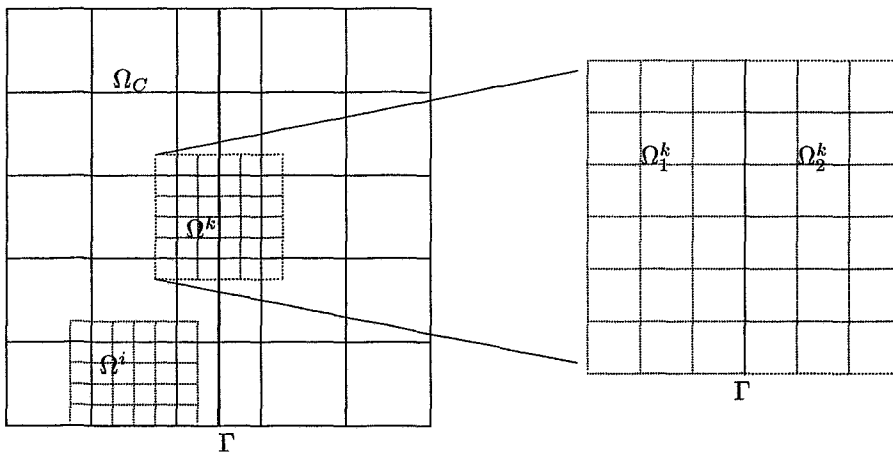


**Figure 2** The coarse grid, and fine overlapping grids.

For those coarse elements that contain an interior boundary we need two additional grids. Let  $\Omega^k$  be a fine grid that contain an interior boundary, then  $\Omega_1^k$  is the part of  $\Omega^k$  that has permeability  $K_1$  and  $\Omega_2^k$  is the part of  $\Omega^k$  that has permeability  $K_2$ .  $\Omega_1^k$  and  $\Omega_2^k$  has equal spacing to  $\Omega^k$ .

## THE SOLUTION PROCEDURE

- Solve the pressure equation, and derive the velocity from the pressure.
- Trace the characteristics with the new velocity.
- Determine the area with large gradients in saturation, and trace the characteristics for the fine grids where the gradients are large.
- if the refined grid has an interior boundary  
   MassBalance iteration.  
   else  
   Solve the elliptic saturation equation.

The three first steps in the procedure is well described and published in [DES92], so we will only describe the new massbalance iteration in the following.

The massbalance iteration ensures that no mass is lost or created at the interior boundary. For the massbalance iteration we use the fine grids which contain an interior

boundary as a control grid. The amount of mass that has been transported in to this "homogeneous" domain,  $\Omega^k$ , is the same mass that we have to distribute between the two subgrids  $\Omega_1^k$  and  $\Omega_2^k$ . The massbalance iteration can be outlined like this:

- Trace the characteristics on  $\Omega_1^k$ .
- Use the jump condition at the boundary,  $P_{C1}(S_1) = P_{C2}(S_2)$ .
- Trace the characteristics on  $\Omega_2^k$ , with the new saturation on the boundary.
- Solve the elliptic equation on  $\Omega_1^k$  and  $\Omega_2^k$  with Diriclet condition at the interior boundary.
- Calculate the massbalance.
- While the mass is not balancing do
  1. Add to the saturation at the left side of the boundary a scaling factor times the error in mass.
  2. Use the jump condition at the boundary to determine the saturation on the right side of the boundary.
  3. Solve the elliptic equation on both domains with the new Diriclet condition at the interior boundary.
  4. Calculate the massbalance.
- end do.

## NUMERICAL RESULTS

The numerical results is shown for two regions with different permeabilities. Figure 4 show the effect of the permeability on the diffusion function.

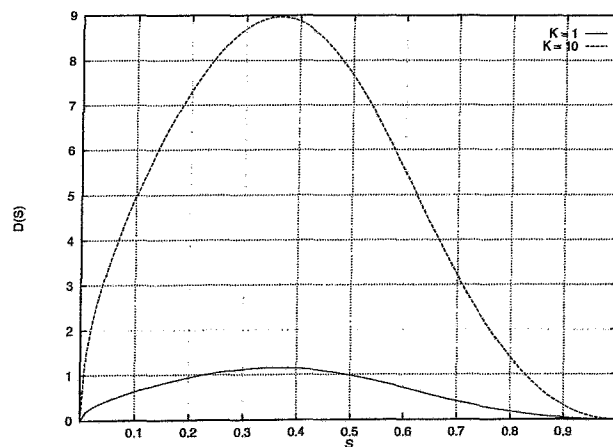
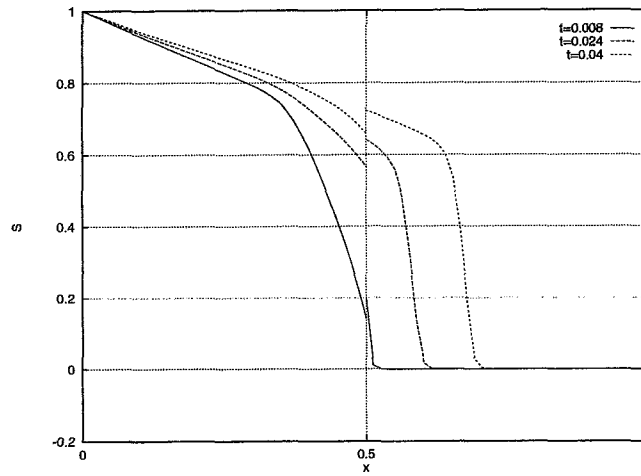


Figure 3 The diffusion function for  $K = 1$  and  $K = 10$ .

The following figures shows a domain with an interface at  $x = 0.5$ . At the interface we have a jump in the saturation profile due to the interface-condition

$$P_{C_1}(S_1) = P_{C_2}(S_2).$$



**Figure 4** Saturation profiles when  $K_1 = 10$  and  $K_2 = 1$ . Interior boundary at  $x = 0.5$  and  $\epsilon = 0.01$ .

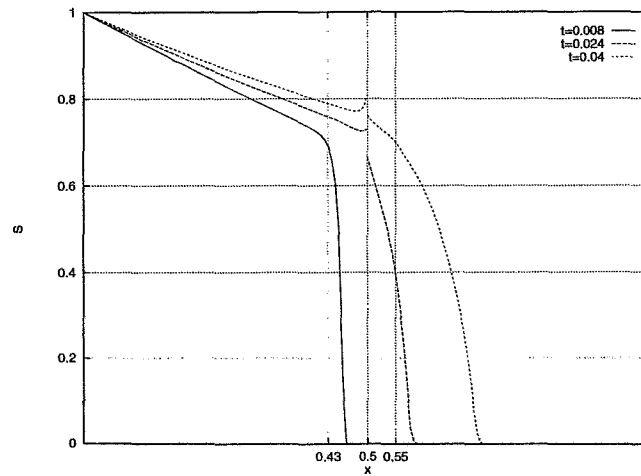


**Figure 5** Saturation profiles when  $K_1 = 1$  and  $K_2 = 10$ . Interior boundary at  $x = 0.5$  and  $\epsilon = 0.01$ .

In 2D the saturation at the interface is given by the mean of the saturation at the interface, therefore we are not able to see the jump as clearly as in 1D, where we were able to present one point with two different saturation values. In both 1D and 2D the mass is nicely conserved. We can conclude that the massbalance iteration work in both 1D and 2D, and is consistent with the boundary conditions 9 and 11. The maximum number of iterations needed in 2D is eleven.

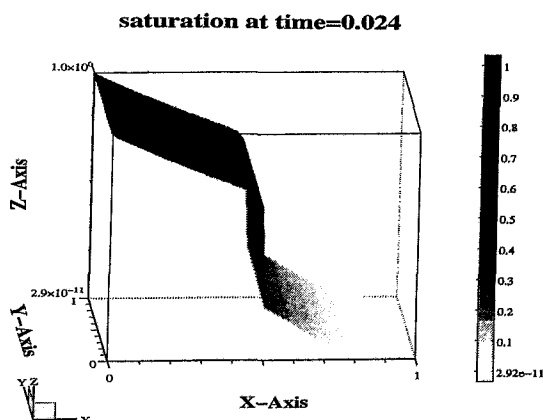


**Figure 6** Saturation profile in 2D when  $K_1 = 1$  and  $K_2 = 10$ . Interior boundary at  $x = 0.5$  and  $\epsilon = 0.01$ .

#### ACKNOWLEDGEMENTS

This research was supported by the Norwegian Research council.

#### REFERENCES

- [BM84] Barrett J. and Morton K. (1984) Approximate symmetrization and petrov-galerkin methods for diffusion-convection problems. *Computer Methods in Applied Mechanics and Engineering* 45: 97-122.
- [DES92] Dahle H., Espedal M., and Sævaerid O. (1992) Characteristic, local grid refinement techniques for reservoir flow problems. *International Journal for Numerical Methods in Engineering* 34: 1051-1069.
- [DR82] Douglas J. and Russell T. (1982) Numerical methods for convection-dominated diffusion problems based on combining the method of characteristics with finite element or finite difference procedures. *SIAM Journal on Numerical*

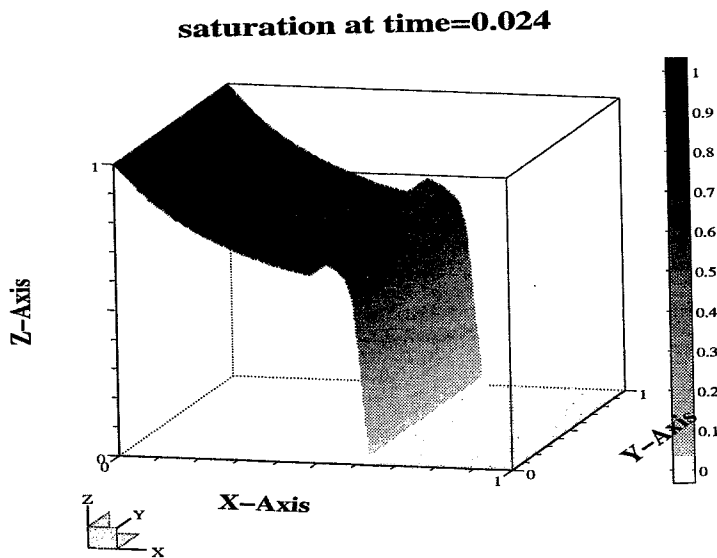


**Figure 7** Saturation profile in 2D when  $K_1 = 10$  and  $K_2 = 1$ . Interior boundary at  $x = 0.5$  and  $\epsilon = 0.01$ .

*Analysis* 19: 871–885.

- [EE87] Espedal M. and Ewing R. (1987) Characteristic petrov-galerkin subdomain methods for two-phase immiscible flow. *Computer Methods in Applied Mechanics and Engineering*. 64: 113–135.
- [KME92] Kristiansen J., Mikkelsen M., and Esbensen K. (1992) A modified leverett approach and pls-regression for integrated formation evaluation. Number 33. Annual Symposium of Society of Professional Well Log Analysis.